Coumarin-Based Thiosemicarbazones: Synthesis, α-Amylase Inhibition and ADMET Analysis

[1]Muhammad Shahid Nazir, [1]Matloob Ahmad*, [2]Azhar Rasul
[1]*Department of Chemistry, Government College University, Faisalabad 38000, Pakistan.*
[2]*Department of Zoology, Baba Guru Nanak University, Nankana Sahib 39100, Pakistan.*
matloob.Ahmad@gcuf.edu.pk*

(Received on 18th September 2025, accepted in revised form 25th October 2025)

Summary: Coumarin derivatives show various pharmaceutical properties, including anti-cancer, anti-bacterial, anti-coagulant, and anti-diabetic. A novel series of coumarin-thiosemicarbazone hybrids was prepared and characterized by using ^1HNMR, mass and IR spectroscopy. The prepared compounds were assessed for their *in vitro* α-amylase inhibitory activity. Among the screened hybrids, Compounds **3c** (IC_{50}= 10.58 ± 0.14 µM) and **3e** (IC_{50}= 9.41 ± 0.15 µM) showed excellent inhibition against α-amylase as compared to the reference drug (acarbose IC_{50}= 16.38 ± 0.17 µM). Molecular docking study indicated that compounds **3c** and **3e** displayed the highest binding scores of -9.2 and -9.3 kcal/mol, respectively, towards the active sites of human pancreatic α-amylase (PDB ID: 2QV4). The acarbose had a binding score of -8.1 kcal/mol. Furthermore, ADMET analysis displayed that these potent derivatives exhibited high oral absorption, compliance with Lipinski's rule, low toxicity predictions, and a promising overall drug-likeness.

Keywords: Coumarin-based thiosemicarbazones, Synthesis, α-Amylase inhibition, Molecular docking, ADMET analysis.

Introduction

Diabetes mellitus (DM) is a chronic metabolic illness that affects billions of people across the world, requiring long-term medical treatment to control blood sugar levels. In diabetes mellitus, glucose accumulates in the bloodstream, resulting in hyperglycemia [1,2]. Hyperglycemia leads to oxidative neuronal damage, while chronic hyperglycemia decreases caloric sugar formation in several organs [3]. The death of beta cells due to genetic problems or autoimmune damage causes Type 1 diabetes (T1DM) [4]. At this stage of disease, people may receive artificial insulin and have a history of insulin-resistant conditions, which often lead to type 2 diabetes [5].

Type 2 diabetes (T2DM) is a metabolic illness that is referred to as a severe chronic health condition. The prevalence of T2DM is rising worldwide day by day due to improper lifestyles such as physical inactivity and poor nutrition. This disease leads to severe health issues, including cardiovascular disease, blindness, kidney failure, and nerve damage [6]. Considering the consequences of currently available medicine, such as harmful side effects and high secondary mortality rates. Medicinal chemists are working for the development of novel pharmaceuticals for the treatment of T2DM. One of the key target is α-amylase enzyme that breaks down carbohydrates, including starches, glycogen, and other polysaccharides, into oligosaccharides, which are further hydrolyzed into monosaccharides by other digestive enzymes [7,8]. Inhibition of α-amylase plays a crucial role in the treatment of diabetes by delaying carbohydrate digestion and reducing postprandial hyperglycemia [5]. Miglitol, acarbose, and voglibose are utilized as α-amylase inhibitors to reduce glucose absorption in the blood [9–11]. These medicines exhibit severe side effects like bloating, diarrhea, and abdominal discomfort in over 20% of diabetic patients [12].

Coumarin family is renowned among natural products as well as synthetic organic compounds [13]. Coumarin and its derivatives are found throughout the tissues of higher plants, including leaves, fruits, roots, and seeds. Coumarin derivatives are also present in bacteria and fungi [14]. Furthermore, the synthesis of novel coumarin hybrids is of great interest to synthetic and medicinal chemists owing to the wide spectrum of pharmaceutical properties [15]. Coumarin derivatives display anti-viral [16], anti-inflammatory [17], anti-microbial [18], anti-coagulant [19], anti-leishmanial [20], anti-cancer [21], and anti-diabetic [22]. Several coumarin based α-amylase inhibitors are mentioned in (Fig. 1).

Schiff bases are an important class of organic molecules containing the azomethine (–HC=N–)

*To whom all correspondence should be addressed.

functional group [23]. The azomethine linkage plays a crucial role in their chemical reactivity and coordination behavior. The electrophilic carbon and nucleophilic nitrogen in the imine linkage (C=N) allow significant interaction ability with various electrophiles and nucleophiles, thereby inhibiting biomolecular targets [24]. Schiff bases exhibit numerous pharmaceutical properties, including anti-microbial [25], anti-inflammatory [26], anti-malarial [27], anti-cancer [28], and anti-diabetic [29]. While, coumarin-based Schiff bases are more attractive due the biological significance of coumarin core. These Schiff bases show anti-bacterial [30], anti-diabetic [31], anti-microbial [32], and anti-cancer [33] activities. Fig. 2 illustrates the structures of Schiff bases and coumarin-based Schiff bases reported as antidiabetic agents. Although several coumarin-thiosemicarbazone hybrids have been reported previously for their α-amylase and α-glucosidase inhibitory potential [34–40]. However, these findings enable us to design more effective α-amylase inhibitors. Hence, we have synthesized structurally diverse novel coumarin-based thiosemicarbazones and evaluated their α-amylase inhibitory activity. Furthermore, molecular docking and ADMET analysis of the prepared derivatives were also performed. Therefore, the novelty of this work lies in the discovery of novel scaffolds with improved inhibitory activity and pharmacokinetic properties.

Experimental

General procedure for the synthesis of coumarin-based thiosemicarbazones **(3a-e)**

3-acetyl-coumarin **1** (0.12 g, 0.0006 moles), various thiosemicarbazides **2a-e** (0.10 g, 0.0005 moles), and 3-4 drops of glacial acetic acid (AcOH) were dissolved in ethanol (20 mL) in a 100 mL round-bottom flask. The reaction was carried out at 90 °C for 2-3 hours under reflux conditions. Upon completion of the reaction (checked by TLC), the precipitated solid was filtered and dried. Finally, the pure products **3a-e** were collected in excellent yields by recrystallization.

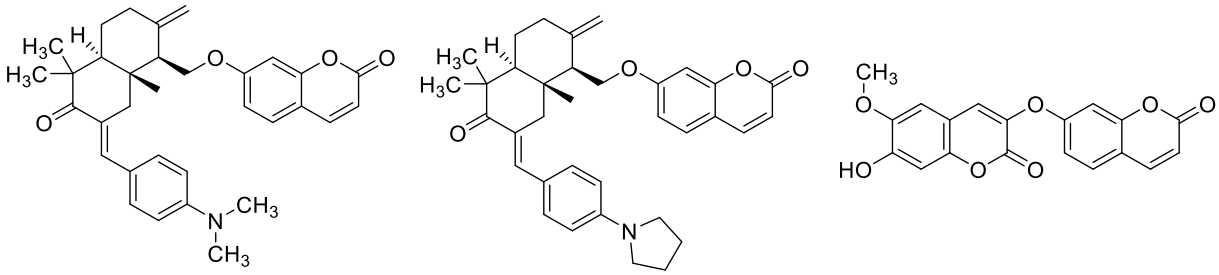

Fig. 1: Structures of coumarin-based scaffolds as α-amylase inhibitors.

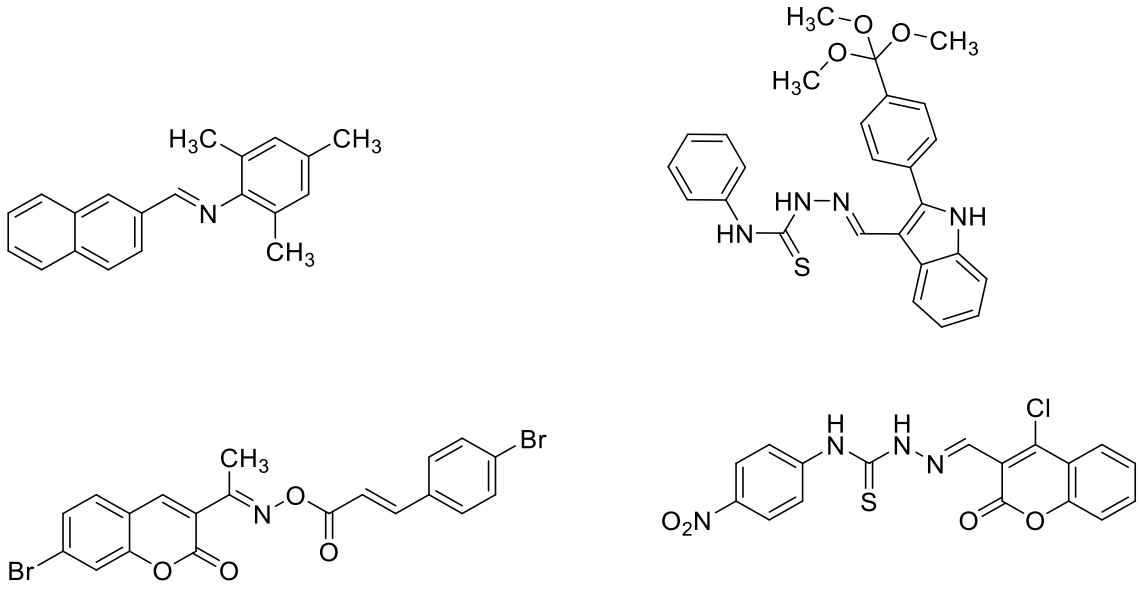

Fig. 2: Structures of Schiff bases and coumarin-based Schiff bases as anti-diabetic agents.

(E)-N-(3-Fluorophenyl)-2-(1-(2-oxo-2H-chromen-3-yl)ethylidene)hydrazine-1-carbothioamide **(3a)**

Yield 81%; M.pt. 240-242 °C. ^{1}HNMR (400 MHz, DMSO-d6): δ (ppm): 2.34 (s, 3H, CH_3), 7.07 – 6.98 (m, 1H), 7.49 – 7.30 (m, 4H), 7.71 – 7.62 (m, 2H), 7.81 (dd, *J* = 7.8, 1.6 Hz, 1H), 8.48 (s, 1H), 10.26 (s, 1H, NH), 11.00 (s, 1H, NH). ^{13}CNMR (100 MHz, DMSO-d6): δ (ppm): 16.1 (CH_3), 111.2 (Ar-C), 115.9 (Ar-2C), 120.7 (Ar-C), 124.7 (Ar-C), 125.3 (Ar-C), 129.2 (Ar-C), 129.6 (Ar-C), 129.7 (Ar-C), 132.5 (Ar-C), 142.3 (Ar-C) 147.0 (Ar-C), 153.3 (C=N), 158.9 (Ar-C), 160.7 (Ar-C), 162.3 (C=O), 176.8 (C=S). LC-MS (ESI): m/z calcd. for $C_{18}H_{14}FN_3O_2S$ $[M-1]^-$ 354.07; found: 354.25. IR (KBr) (ν_{max}, cm^{-1}): 3224.5 (NH-str.), 3061.2 (NH-str.), 1703.6 (C=O str. of coumarin ester), 1609.4 (C-H of phenyl), 1597.4 (C=N str.), 1547.4 (N-H bend), 1488.5 (C=C str. of aromatic ring), 1438.4 (CH_3-asym. bend), 1383.8 (CH_3-sym. bend), 1308.5 (C-N str.), 1199.5 (C=S str.), 1262.4 (C-O-C str.), 1153.8 (C-O str.), 948 (N-H str.).

(E)-N-(4-Fluorophenyl)-2-(1-(2-oxo-2H-chromen-3-yl)ethylidene)hydrazine-1-carbothioamide **(3b)**

Yield 87%; M.pt. 233-235 °C. ^{1}HNMR (400 MHz, DMSO-d6): δ (ppm): 2.33 (s, 3H, CH_3), 7.18 (dtd, *J* = 8.8, 7.0, 2.2 Hz, 3H), 7.46 – 7.44 (m, 2H), 7.57 (d, *J* = 3.7 Hz, 1H), 7.68 – 7.65 (m, 1H), 7.80 (dd, *J* = 7.8, 1.6 Hz, 1H), 8.49 (s, 1H), 10.14 (s, 1H, NH), 10.87 (s, 1H, NH). LC-MS (ESI): m/z calcd. for $C_{18}H_{14}FN_3O_2S$ $[M+1]^+$ 356.08; found 356.16. IR (KBr) (ν_{max}, cm^{-1}): 3256.7 (NH-str.), 3210.5 (NH-str.), 1709.2 (C=O str. of coumarin ester), 1625.6 (C-H of phenyl), 1598.4 (C=N str.), 1534.1 (N-H bend), 1493.8 (C=C str. of aromatic ring), 1435.6 (CH_3-asym. bend), 1320.7 (C-N str.), 1180.4 (C=S str.), 1269.3 (C-O-C str.), 1130.4 (C-O str).

(E)-N-(4-Ethylphenyl)-2-(1-(2-oxo-2H-chromen-3-yl)ethylidene)hydrazine-1-carbothioamide **(3c)**

Yield 85%; M.pt. 205-207 °C. ^{1}HNMR (400 MHz, DMSO-d6): δ (ppm): 1.19 (t, *J* = 7.6 Hz, 3H, CH_3), 2.33 (s, 3H, CH_3), 2.64 – 2.53 (m, 2H, CH_2), 7.23 – 7.16 (m, 2H), 7.40 (tdd, *J* = 7.5, 4.0, 1.1 Hz, 1H), 7.50 – 7.43 (m, 3H), 7.67 (dddd, *J* = 10.0, 8.7, 7.3, 1.6 Hz, 1H), 7.78 (ddd, *J* = 18.4, 7.7, 1.6 Hz, 1H), 8.49 (s, 1H), 10.08 (s, 1H, NH), 10.80 (s, 1H, NH). LC-MS (ESI): m/z calcd. for $C_{20}H_{19}N_3O_2S$ $[M-1]^-$ 364.11; found 364.08. IR (KBr) (ν_{max}, cm^{-1}): 3220.1 (NH-str.), 3035.7 (NH-str.), 1719.2 (C=O str. of coumarin ester), 1610.1 (C-H of phenyl), 1585.4 (C=N str.), 1530.1 (N-H bend), 1501.1 (C=C str. of aromatic ring), 1434.1 (CH_3-asym. bend,) 1396.3 (CH_3-sym. bend), 1312.3 (C-N str.), 1255.1 (C-O-C str.), 1191.3 (C=S str.), 1150.3 (C-O str.), 956.2 (N-H str).

(E)-N-(2-Chlorophenyl)-2-(1-(2-oxo-2H-chromen-3-yl)ethylidene)hydrazine-1-carbothioamide **(3d)**

Yield 82%; M.pt. 251-253 °C. ^{1}HNMR (400 MHz, DMSO-d6): δ (ppm): 2.35 (s, 3H, CH_3), 7.25 (dddd, *J* = 18.9, 8.1, 2.2, 1.0 Hz, 1H), 7.44 – 7.34 (m, 2H), 7.46 (t, *J* = 7.8 Hz, 1H), 7.62 – 7.57 (m, 1H), 7.71 – 7.64 (m, 1H), 7.84 – 7.79 (m, 2H), 8.48 (s, 1H), 10.24 (s, 1H, NH), 11.02 (s, 1H, NH). LC-MS (ESI): m/z calcd. for $C_{18}H_{14}ClN_3O_2S$ $[M-1]^-$ 370.04; found 370.17. IR (KBr) (ν_{max}, cm^{-1}): 3229 (NH-str.), 3084.4 (NH-str.), 1706.4 (C=O str. of coumarin ester), 1613.3 (C-H of phenyl), 1593.6 (C=N str.), 1534.7 (N-H bend), 1497.3 (C=C str. of aromatic ring), 1434 (CH_3-asym. bend), 1388.3 (CH_3-sym. bend), 1312.3 (C-N str.), 1186.8 (C=S str.), 1262.2 (C-O-C str.), 1148.8 (C-O str.), 951.8 (N-H str).

(E)-N-(3-Chlorophenyl)-2-(1-(2-oxo-2H-chromen-3-yl)ethylidene)hydrazine-1-carbothioamide **(3e)**

Yield 79%; M.pt. 244-246 °C. ^{1}HNMR (400 MHz, DMSO-d6): δ (ppm): 2.35 (s, 3H, CH_3), 7.32 (dd, *J* = 7.8, 1.7 Hz, 1H), 7.41 – 7.37 (m, 2H), 7.45 (d, *J* = 8.5 Hz, 1H), 7.53 (ddd, *J* = 15.1, 8.0, 1.5 Hz, 1H), 7.67 – 7.65 (m, 1H), 7.76 (ddd, *J* = 12.3, 7.9, 1.7 Hz, 2H), 8.48 (s, 1H), 10.10 (s, 1H, NH), 11.03 (s, 1H, NH). LC-MS (ESI): m/z calcd. for $C_{18}H_{14}ClN_3O_2S$ $[M-1]^-$ 370.04; found 370.08. IR (KBr) (ν_{max}, cm^{-1}): 3261.7 (NH-str.), 3215.5 (NH-str.), 1718.1 (C=O str. of coumarin ester), 1629.1 (C-H of phenyl), 1596.4 (C=N str.), 1547.4 (N-H bend), 1497.3 (C=C str. of aromatic ring), 1438.6 (CH_3-asym. bend), 1316.8 (C-N str.), 1182.4 (C=S str.), 1260.3 (C-O-C str.), 1132.8 (C-O str.), 968 (N-H str).

In Silico α-Amylase Inhibition

Preparation of target protein and ligands

The 3D crystal structure of human pancreatic α-amylase (PDB ID: 2QV4) was downloaded from protein data bank (https://www.rcsb.org/). Solvent molecules and dummy atoms were removed from the protein using UCSF Chimera 1.16. The structures of each prepared molecule were sketched using ChemDraw Ultra 12.02 and saved as an SD file (".sdf") to open in PyRx software. The structure of reference drug (acarbose) was retrieved from NCBI Pubchem. Chimera tool was also utilized to minimize the energy of all the ligands, acarbose, and the receptor protein.

Molecular docking

Molecular docking analysis was conducted by utilizing Auto Dock Vina of PyRx software [41]. The selection of the grid box around the active sites of receptor protein is crucial. The grid box with coordinates X=17.4491, Y=61.8955, and Z=15.8297, along with dimensions (in angstroms) of X=57.9134, Y=73.9404, and Z=59.1041, was created to cover binding pockets of protein. Each ligand was docked with (PDB ID: 2QV4) protein to evaluate docking scores and binding interactions. Ligand-protein complexes were saved in pdbqt format. Finally, discovery Studio (DS) visualizer was utilized to observe the interaction modes between ligand and protein [42].

In vitro α-Amylase Inhibition Assay

A previously described method with slight modifications was used to examine the inhibition activity of all prepared derivatives and acarbose against the α-amylase enzyme [43]. 40 µL of each test sample was filled into 96-well microliter plates. Then, 40 µL solution of α-amylase (*Aspergillus oryzae*, Sigma-Aldrich) prepared in phosphate buffer (0.02 M, pH = 6.9) was added into it and incubated at 37°C for 10 minutes. After incubation, each well was filled with a solution of 40 µL starch (prepared in 20mM phosphate buffer, pH 6.9) as a substrate and kept at 37 °C for 20-30 minutes. After that, 3,5-dinitrosalicylic acid (100 µL) was added and the mixture was placed in hot water for 5 minutes at 95 °C. Finally, the distilled water (400 µL) was used to dilute the solution. The absorbance was measured at a 540 nm wavelength. Standard and negative inhibitors were acarbose (Sigma-Aldrich) and DMSO, respectively. The assay was performed in triplicate to calculate the percentage inhibition values.

$$\%\text{Inhibition} = [(A_{control}-A_{sample})/A_{control}] \times 100$$

where A is absorbance.

Statistical Data

The IC_{50} values of each compound were calculated by using Graph Pad Prism 7.0 (Graph Pad Software Inc., CA, and USA). All data were described as mean ± SD. One-way ANOVA was performed to find the difference between groups. $P < 0.05$ was considered significant.

ADMET analysis

Drug-likeness and ADMET properties of the most potent derivatives **3c** and **3e** were evaluated by employing PreADMET online server [44].

Results and Discussion

Chemistry

Coumarin-thiosemicarbazones **3a-e** were synthesized by the coupling of 3-acetyl coumarin **1** and various thiosemicarbazides **2a-e** using acetic acid (AcOH) as a catalyst in ethanol solvent at 90 °C for 2-3 hours under reflux. The progress of reaction was continuously monitored by TLC. The resulting precipitates were filtered, washed with distilled water and methanol. Pure products **3a-e** were achieved in excellent yields by recrystallization with chloroform (Scheme 1).

All the synthesized compounds were characterized by using ^{1}HNMR, mass and IR spectroscopic techniques. In ^{1}HNMR spectra, protons of methyl (CH_3) group were given a singlet at 2.33-2.35 ppm [39,40]. The aromatic protons were observed at 7.19-8.49 ppm. Similarly, NH proton was spotted as a singlet at 10.08-11.03 ppm [47]. At 1.19 ppm, methyl (CH_3) protons of the ethyl ($-CH_2CH_3$) group were attributed as a triplet, while CH_2 protons were observed as a multiplet at 2.53-2.64 ppm [48]. In ^{13}CNMR spectrum of compound **3a**, the methyl carbon appeared at 16.1 ppm [49]. The carbon atoms of coumarin and phenyl rings were observed at 111.2-158.9 ppm. The peak at 162.3 was attributed to carbonyl carbon (C=O). The carbon atoms of C=N and C=S group were observed at 160.7 ppm and 176.8 ppm [50]. In LC-MS spectra, $[M-1]^-$ and $[M+1]^+$ peaks were observed. In IR spectra, the stretching peaks of N-H and C=O (coumarin ester) appeared in the region of 3035.7-3261.7, and 1703.6-1719.2 cm^{-1} [1]. The C=N and C=S stretching peaks appeared at 1585.4-1597.4, and 1182.4-1199.5 cm^{-1}, respectively [31]. The stretching peaks of C-O-C and C-O were observed at 1255.1-1262.4 and 1130.4-1153.8 cm^{-1}. The absorption bands of C-H, and C=C appeared at 1609.4-1629.1, and 1488.5-1501.1 cm^{-1}, respectively [51]. The asymmetric and asymmetric stretching vibrations of methyl group (CH_3) appeared at 1434.1-1438.6 and 1383.8-1396.3 cm^{-1}, respectively. The N-H bending vibrations appeared at 1530.1-1547.4 cm^{-1}, while C-N stretching vibrations appeared at 1308.5-1316.8 cm^{-1} [52]. The representative ^{1}HNMR, ^{13}CNMR, mass, and IR spectra of compound **3a** are given in (Fig. 3-6)

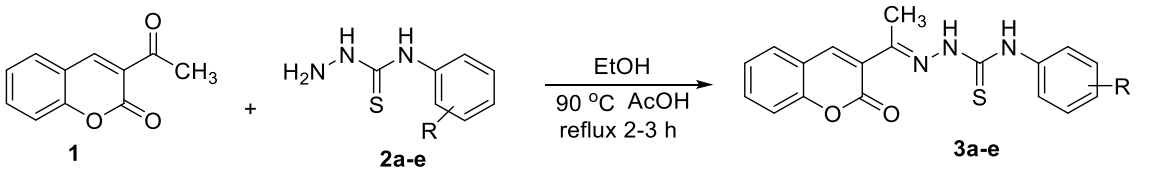

R= **3a,** 3-F, **3b,** 4-F, **3c,** 4-Et, **3d,** 2-Cl, **3e,** 3-Cl

Scheme-1: Synthesis of novel coumarin-based thiosemicarbazones.

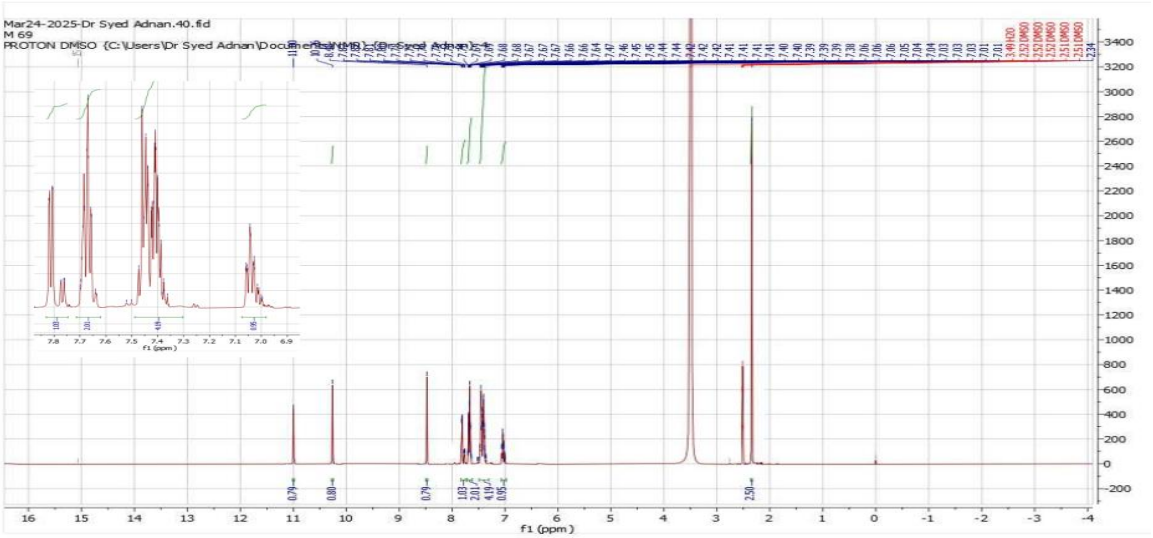

Fig. 3: The ^{1}H NMR spectrum of a representative compound **3a.**

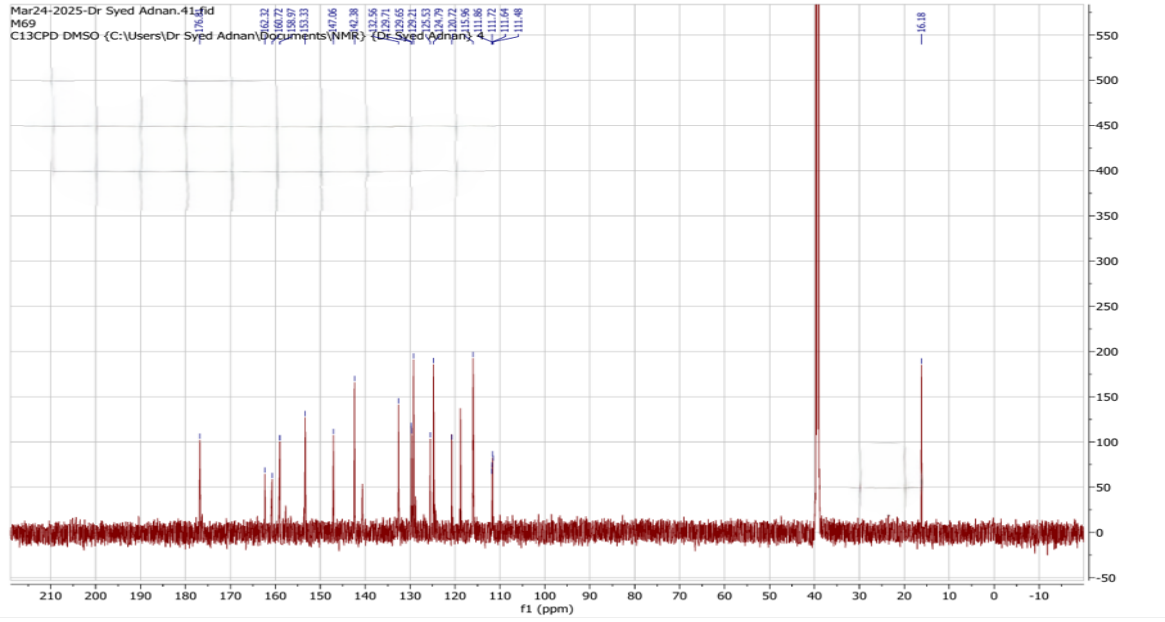

Fig. 4: The ^{13}C NMR spectrum of compound **3a.**

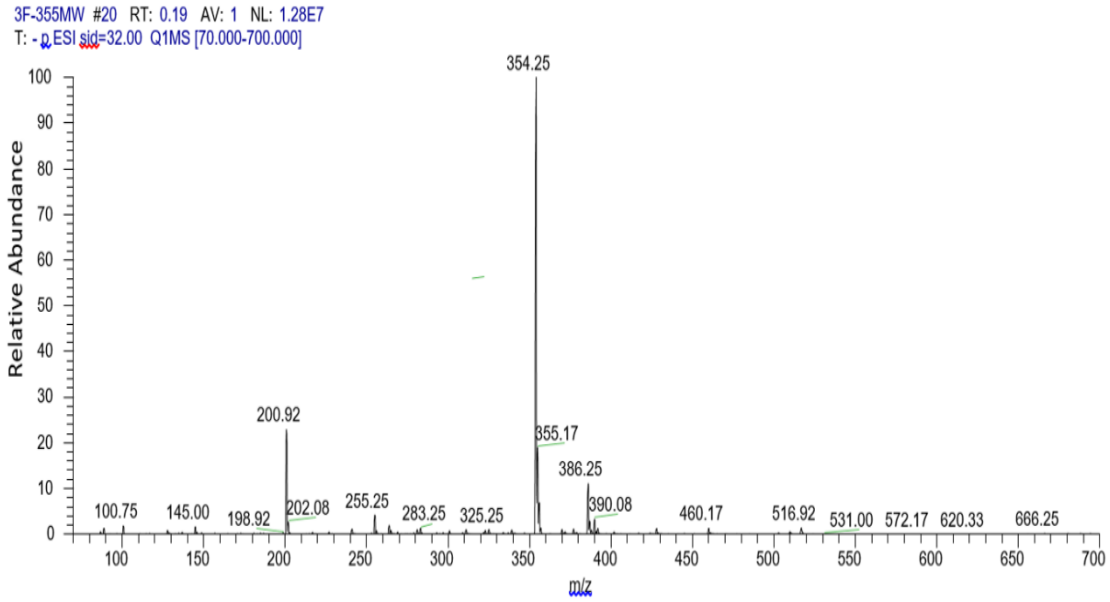

Fig. 5: The Mass Spectrum of compound **3a.**

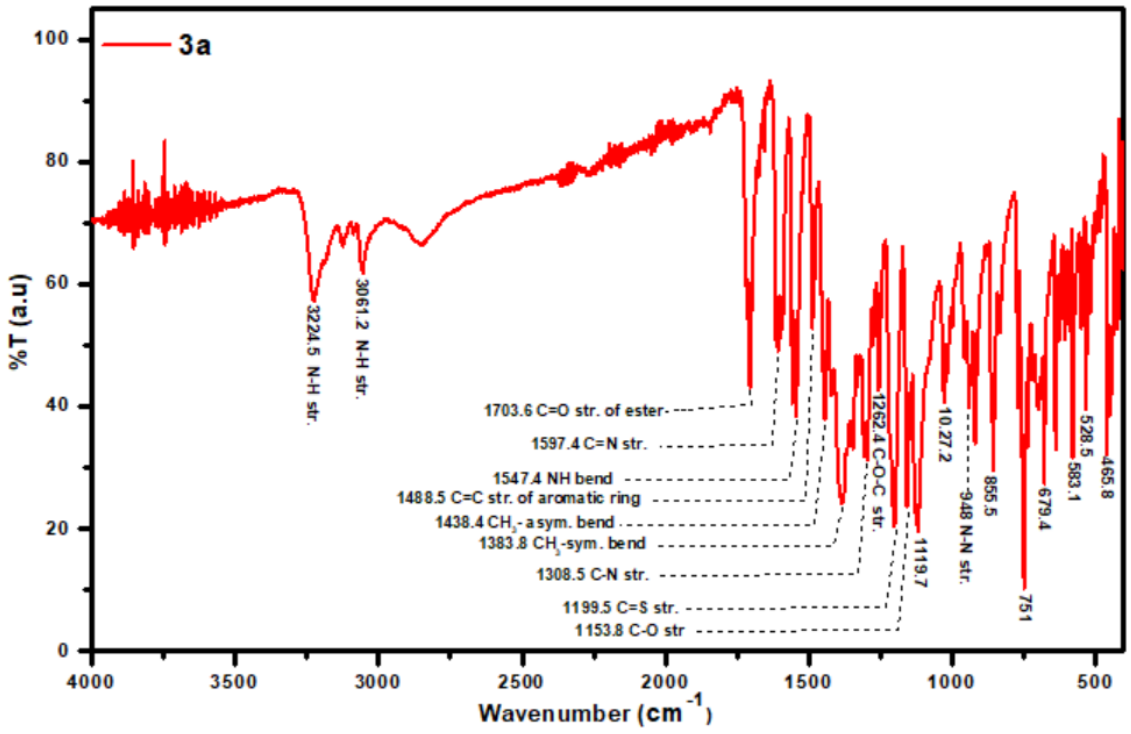

Fig. 6: The IR spectrum of compound **3a.**

In silico analysis (α-amylase inhibition)

Molecular docking is an excellent strategy for discovering biologically useful compounds that eliminate demand for manual synthesis. Therefore, molecular docking of all derivatives 3a-e and reference drug (acarbose) was performed against human pancreatic α-amylase (PDB ID: 2QV4) to evaluate the binding scores and interaction modes, as shown in Tables 1 and 2. Acarbose, with a binding score (-8.1 kcal/mol), formed hydrogen bonding interactions with TYR62, THR163, ASP197, HIS201, and GLU233 (Fig. 7).

Compound **3c** demonstrated an excellent binding score of (-9.2 kcal/mol) (table 2). ALA198 formed carbon-hydrogen bond with the O-atom of coumarin ring. Furthermore, the sulfur atom of the thiosemicarbazide moiety exhibited π-sulfur interactions with TRP58, TYR62, and HIS299. Amino acid residues: TRP59, LEU162, LEU165, LYS200, HIS201, and ILE235 formed π-π stacked, π-π T-shaped, and π-alkyl interactions with *N*-phenyl and coumarin rings. In addition, the coumarin ring also displayed π-anion interaction with GLU233. Moreover, *N*-phenyl ring of derivative **3c** bearing an ethyl group at the *para*-position displayed π-alkyl interaction with TRP59 (Table 1, Fig. 7).

On the other hand, compound **3e** was found to be the most potent among the series of coumarin-thiosemicarbazone hybrids with the highest binding score (-9.3 kcal/mol) (Table 2). The NH group of thiosemicarbazide moiety displayed conventional hydrogen bonding with ASP300. Amino acid residues: TRP59 and HIS201 formed π-π T-shaped and π-π stacked interactions with coumarin and *N*-phenyl rings. Additionally, the chloro group attached at the *meta*-position of the *N*-phenyl ring exhibited π-alkyl interactions with TYR151 and HIS201, respectively. Furthermore, the *N*-phenyl ring of this ligand also demonstrated π-alkyl interactions with LYS200 and ILE235, respectively (Fig. 7).

α-Amylase is a key enzyme that breaks down α-1,4-glycosidic bonds in polysaccharides such as starch and glycogen [53]. Three major catalytic residues, ASP197, GLU233, and ASP300, are located within the binding pocket of the enzyme and are crucial for the cleavage of the α-1,4-glycosidic linkage. ASP197 (serves as a nucleophile) attacks the glycosidic bond in the substrate to afford the formation of a covalent glycosyl–enzyme intermediate. GLU233 acts as an acid-base catalyst. It facilitates the bond cleavage by donating a proton to the glycosidic oxygen and subsequently hydrolyze the intermediate to release the product by accepting a proton from a water molecule. ASP300 stabilizes the transition state and properly aligns the catalytic residues and substrates by retaining the electrostatic environment and correct geometry within the binding pocket. Along with the catalytic residues, several other amino acid residues such as TRP58, TRP59, TYR62, TYR151, HIS201, LYS200, ILE235, LEU162, LEU165, ALA198, and HIS299 involves in stabilization and substrate binding [54]. Therefore, coumarin-based thiosemicarbazones **3c** and **3e** interact with catalytic and binding site amino acid residues *via* hydrogen bonding and hydrophobic interactions, stabilizing the enzyme-inhibitor complex and thereby increasing the α-amylase inhibitory potential.

Table-1: Ligand-protein binding interactions of 3c and 3e with active sites of human pancreatic α-amylase (PDB ID: 2QV4).

	Hydrogen bonding interactions		Hydrophobic interactions		Electrostatic interactions	
Compounds	**Amino acid residues**	**interactions**	**Amino acid residues**	**interactions**	**Amino acid residues**	**interactions**
3c	**ALA198**	**Carbon H-bonding**	**TRP59 and HIS201**	**π-π Stacked and π-π T shaped**	**GLU233**	**π-Anion**
			LEU162, LEU165, LYS200 and ILE235	**π-Alkyl**	**TRP58, TYR62 and HIS299**	**π-Sulfur**
3e	**ASP300**	**Conventional H-bonding**	**TRP59 and HIS201**	**π-π T shaped and π-π Stacked**	**-**	**-**
			TYR151, LYS200 and ILE235	**π-Alkyl**	**-**	**-**
Acarbose		**Conventional H-bonding**	**TYR62, THR163, ASP197, HIS201, and GLU233**	**-**	**-**	**-**

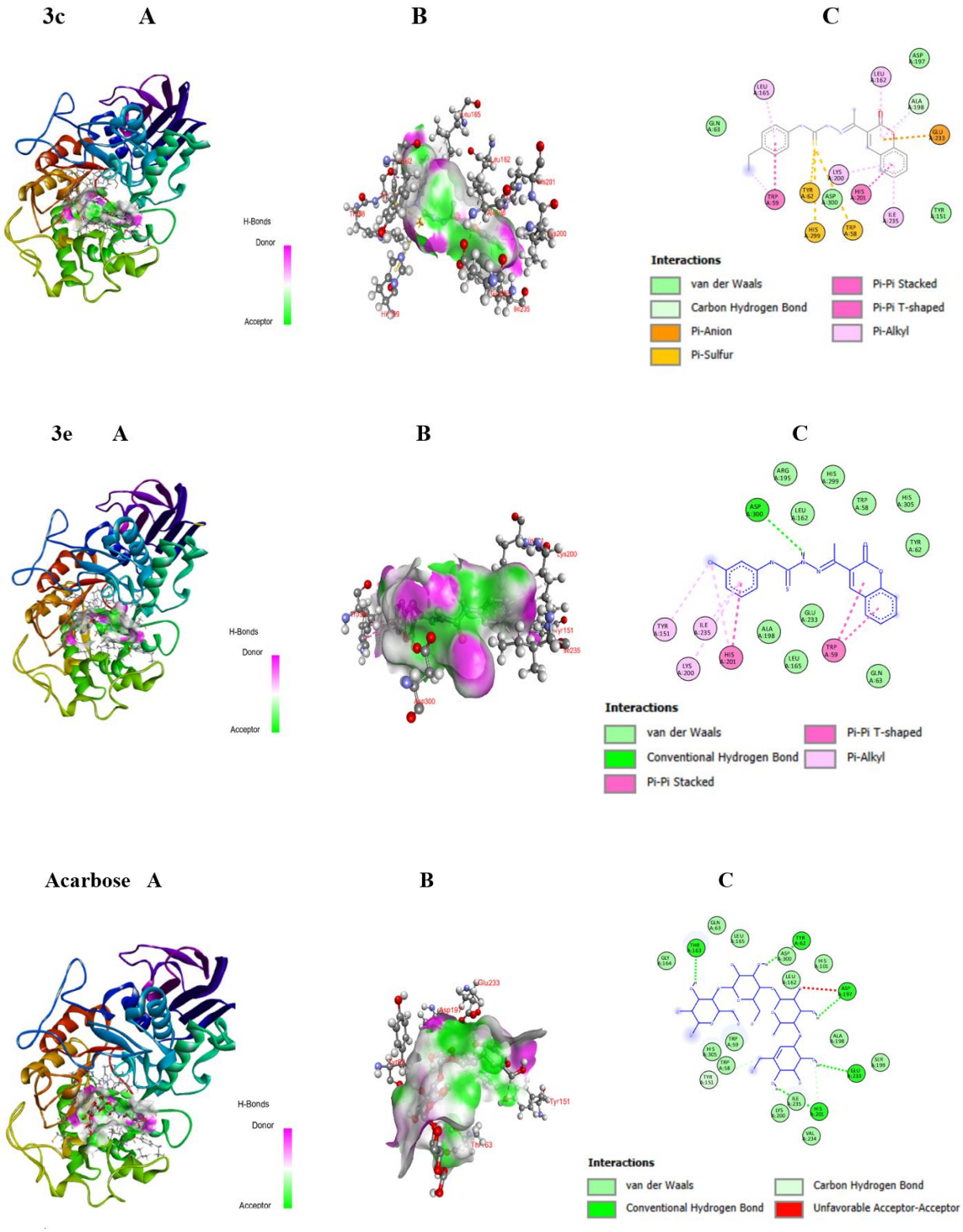

Fig. 7: (A and B) 3D binding interactions of **3c**, **3e** and acarbose with 2QV4 receptor protein. (C) 2D representation of binding analysis of **3c**, **3e**, and acarbose with 2QV4 receptor protein.

In vitro analysis (α-amylase inhibition)

All the synthesized hybrids were assessed *via in vitro* analysis against α-amylase (*Aspergillus oryzae*). The IC_{50} value of acarbose were observe as 16.38 ± 0.17 µM. The prepared hybrids with substituents (3-F, 4-F, 4-Et, 2-Cl, and 3-Cl) exhibited different inhibition activity against α-amylase. The obtained *in vitro* results are mentioned in Table 2.

Structure-activity relationship described that the incorporation of electron-donating (ethyl), and electron-withdrawing (F and Cl) groups on the *N*-phenyl ring showed better α-amylase inhibition than acarbose. In addition, the position of different substituents (F, Et, Cl) showed a profound influence on enzyme inhibition. In general, all the prepared coumarin-based thiosemicarbazones displayed different α-amylase inhibition with remarkable efficacy. The prepared hybrids inhibited α-amylase with IC_{50} values ranging from 9.41 ± 0.15 to 13.86 ± 0.19 µM. Among the synthesized compounds, hybrid **3e** bearing an electron-withdrawing group (Cl) at the *meta*-position of the *N*-phenyl ring was found to be the most potent and efficient inhibitor of α-amylase with an IC_{50} value of 9.41 ± 0.15 µM. Hybrid **3c** also exhibited good inhibitory activity against α-amylase when the ethyl group was substituted at the *para*-position of the *N*-phenyl ring, with an IC_{50} value of 10.58 ± 0.14 µM. Furthermore, adding a chloro group to the *ortho*-position of the aforementioned ring in hybrid **3d** led to a decrease in α-amylase inhibition with an IC_{50} value of 13.86 ± 0.19 µM. Similarly, Compounds **3a** (IC_{50}= 12.36 ± 0.18 µM) and **3b** (IC_{50}= 13.24 ± 0.12 µM), containing a fluoro group at *meta*- and *para*-positions of the *N*-phenyl ring, showed significant inhibitory activity against α-amylase.

In vitro analysis predicted that, compound **3e** was found to be more potent against α-amylase than the coumarin-thiosemicarbazone hybrids previously reported in the literature. For example, Celik *et al*., [38] prepared a series of coumarin-thiosemicarbazone-based metal complexes and evaluated for their anti-diabetic activity. Among them, coumarin-thiosemicarbazone zinc (II) complex showed good α-amylase inhibition with an IC_{50} value of 13.72 µM. A novel series of 3-acetyl-8-ethoxy coumarin-derived thiosemicarbazones was synthesized by Zareen *et al*., [40] and screened for their α-amylase inhibitory activity. From these, (*E*)-2-[1-(8-methoxy-2-oxo-2*H*-chromen-3-yl)ethylidene]hydrazine-1-carbothioamide showed highest α-amylase inhibitory activity with an IC_{50} value of 73.68 ± 2.84 µM.

Table-2: *In silico* (binding scores) and *in vitro* (IC_{50} SEM±µM) analysis of all ligands and acarbose.

Sr. No	Substituents	Binding scores (kcal/mol)	IC_{50} (SEM±µM)
3a	**3-F**	**-9.1**	**12.36±0.18**
3b	**4-F**	**-9.0**	**13.24±0.12**
3c	**4-Et**	**-9.2**	**10.58±0.14**
3d	**2-Cl**	**-9.0**	**13.86±0.19**
3e	**3-Cl**	**-9.3**	**9.41±0.15**
acarbose	**-**	**-8.1**	**16.38±0.17**

ADMET profiling

Drug-likeness and ADMET properties of potent compounds **3c** and **3e** were executed by using PreADMET online server. The obtained results are presented in Table 3. This table indicates that compounds **3c** and **3e** followed Lipinski's Rule of Five. Both compounds were found to be inhibitors of P-glycoprotein. Inhibition of P-glycoprotein increases the retention time of active compounds in target tissues. These ligands also exhibited moderate permeability to Caco-2 cells. Caco-2 permeability indicates the potential of active compounds to pass through the intestinal epithelial cells. The high human intestinal absorption (HIA) scores of active compounds **3c** and **3e** indicated that they can be easily absorbed in the human intestine. Furthermore, the ligands **3c** and **3e** showed high plasma protein binding ability and blood-brain barrier (BBB) permeability. Blood-brain barrier (BBB) permeability determines the ability of compounds to cross the central nervous system (CNS). For CYP2D6 enzyme, both potent compounds were non-inhibitors and non-substrates. These compounds were also found to be non-inhibitors and substrates of cytochrome P450 (CYP3A4) enzyme. CYP2D6 and CYP3A4 enzymes play a crucial role in the oxidative metabolism of pharmaceutically active compounds in the liver. Non-inhibition of CYP2D6 predicts a lower risk of metabolic disorders associated with genetic mutations, while non-inhibition of CYP3A4 suggests the active compounds are less likely to cause drug-drug interactions. AMES toxicity results revealed that compounds **3c** and **3e** were mutagenic. Additionally, *in silico* ADMET analysis, these compounds showed a negative carcinogenic effect in rats and a positive carcinogenic effect in mice. In terms of cardiotoxicity (hERG inhibition), both compounds showed moderate risk of cardiovascular diseases. Overall, these results show the favorable physiochemical and pharmacokinetic properties of the coumarin-based thiosemicarbazones **3c** and **3e**.

Table-3: ADMET profiling of the potent compounds **3c** and **3e**.

Lipinski's rule of five	Compound 3c	Compound 3e
	Favorable	Favorable
Absorption		
HIA	**95.3745**	**95.7712**
Caco2	**22.582**	**23.9497**
Pgp Inhibitor	**inhibitor**	**inhibitor**
Distribution		
BBB	**1.4528**	**1.0715**
PPB	**93.0986**	**94.2494**
Metabolism		
CYP2D6 inhibitor	**Non- inhibitor**	**Non- inhibitor**
CYP2D6 substrate	**Non-substrate**	**Non-substrate**
CYP3A4 inhibitor	**Non-inhibitor**	**Non-inhibitor**
CYP3A4 substrate	**substrate**	**substrate**
Toxicity		
AMES Toxicity	**Mutagen**	**Mutagen**
Carcino Rat	**Negative**	**Negative**
Carcino Mouse	**Positive**	**Positive**
hERG inhibition	**Moderate risk**	**Moderate risk**

Lipinski's rule of five= MW ≤ 500, HBA ≤ 10, HBD ≤ 5 and Clog P ≤ 5

HIA= Low absorption: 0–20%, Moderate absorption: 20-70%, High absorption: 70-100%

CaCO2: Low permeability: < 4, Moderately permeability: 4-70%, High permeability: > 70%

BBB= CNS- Inactive compounds < 1, CNS-active compounds > 1

PPB= Low: < 90%, High: > 90%

Conclusion

We have described the synthesis and α-amylase inhibition of (*E*)-2-(1-(2-oxo-2*H*-chromen-3-yl)ethylidene)-*N*-phenylhydrazine-1-carbothioamides **3a-3e**. *In vitro* study indicated that all the derivatives showed good inhibitory potential in comparison to the reference drug (acarbose, IC_{50}= 16.38 ± 0.17). Compounds **3c** and **3e**, having an electron-donating group (ethyl) and an electron-withdrawing group (chloro) at *para* and *meta*-positions of the *N*-phenyl ring, were found to be good inhibitors of α-amylase (*Aspergillus oryzae*) with IC_{50} values of 10.58 ± 0.14 and 9.41 ± 0.15 µM, respectively. In addition, molecular docking analysis was carried out to assess binding scores and interaction modes of all ligands with the receptor protein. ADMET analysis was conducted to predict the physicochemical and pharmacokinetic properties of the potent coumarin-based thiosemicarbazones **3c** and **3e**. Hence, the present work would be valuable for synthetic and medicinal chemists in the development of novel α-amylase inhibitors for the treatment of diabetes mellitus.

Acknowledgement

The authors are grateful to Government College University, Faisalabad and Higher Education Commission of Pakistan for financial support.

References

1. D. R. Niri, M. H. Sayahi, S. Behrouz, A. Moazzam, S. Mojtabavi, M. A. Faramarzi and M. Mahdavi, Design, Synthesis, *In Vitro*, and *In Silico* Biological Evaluations of Coumarin-indole Hybrids as New Anti-α-glucosidase Agents, *BMC Chemistry*., **16**, 84 (2022).
2. M. Adib, F. Peytam, M. R. Jazi, M. M. Khanaposhtanib, S. Mahernia, H. R. Bijanzadeh and B. Larijani, Design, Synthesis, *In Vitro* α-Glucosidase Inhibition, Molecular Modeling, and Kinetic Study of Novel Coumarin Fused Pyridine Derivatives as Potent Antidiabetic Agents, *New J. Chem*., **42**, 17268 (2018).
3. F. A. Saddique, M. Ahmad, U. A. Ashfaq, M. Muddassar, S. Sultan, and M. E. A. Zaki, Identification of Cyclic Sulfonamides with an N-Arylacetamide Group as α-Glucosidase and α-Amylase Inhibitors: Biological Evaluation and Molecular Modeling, Pharmaceuticals., 15, 106 (2022).
4. R. Ichale, A. M. Kanhed and A. Vora, Coumarin Linked Thiazole Derivatives as Potential α-Glucosidase Inhibitors to Treat Diabetes Mellitus, *Mol. Divers*., **28**, 1239 (2024).
5. W. Baccari, I. Saidi, I. Filali, M. Znati, H. Lazrag, M. Tounsi and H. B. Jannet, Semi-Synthesis, α-Amylase Inhibition, and Kinetic and Molecular Docking Studies of Arylidene-Based Sesquiterpene Coumarins Isolated from Ferula Tunetana Pomel ex Batt, *RSC Advances*., **14**, 4654 (2024).
6. F. Khan, A. A. Shah, A. Kumar and S. Akhtar, *In Silico* Investigation Against Inhibitors of Alpha-Amylase Using Structure-Based Screening, Molecular Docking, and Molecular Simulations Studies, *Cell. Biochem. Biophys*., **82**, 2873 (2024).
7. A. M. Brzozowski and G. J. Davies, Structure of the *Aspergillus Oryzae* α-Amylase Complexed with the Inhibitor Acarbose at 2.0 Å Resolution, *Biochem*., **36**, 10837 (1997).
8. P. M. de Souza, Application of Microbial α-Amylase in Industry-A Review, *Braz. J. Microbiol*., **41**, 850 (2010).
9. A. A. Adegboye, K. M. Khan, U. Salar, S. A. Aboaba, S. Chigurupati, I. Fatima and S. Perveen, 2-Aryl Benzimidazoles: Synthesis, *In Vitro* α-Amylase Inhibitory Activity, and Molecular Docking Study, *Eur. J. Med. Chem*., **150**, 248 (2018).
10. M. Sherafati, M. M. Khanaposhtani, S. Moradi, M. S. Asgari, N. Najafabadipour, M. A. Faramarzi, M. H Hajimiri, Design, Synthesis and Biological Evaluation of Novel Phthalimide-

Schiff Base-Coumarin Hybrids as Potent α-Glucosidase Inhibitors, *Chem. Pap*., **74**, 4379 (2020).
11. A. K. Maurya, V. Mulpuru and N. Mishra, Discovery of Novel Coumarin Analogs Against the α-Glucosidase Protein Target of Diabetes Mellitus: Pharmacophore-Based QSAR, Docking, and Molecular Dynamics Simulation Studies, *ACS Omega*., **5**, 32234 (2020).
12. F. A. Saddique, S. Aslam, M. Ahmad, U. A. Ashfaq, M. Muddassar, S. Sultan and M. E. Zaki, Synthesis and α-Glucosidase Inhibition Activity of 2-[3-(Benzoyl/4-Bromobenzoyl)-4-Hydroxy-1,1-Dioxido-2*H*-Benzo [*e*][1,2]Thiazin-2-yl]-*N*-Arylacetamides: An *In Silico* and Biochemical Approach, *Molecules*., **26**, 3043 (2021).
13. R. D. H, Murray Coumarins, *Nat. Prod. Rep*., **12**, 477 (1995).
14. S. D. Sarker and L. Nahar, Progress in the Chemistry of Naturally Occurring Coumarins. *Prog. Chem. Org. Nat. Prod*., **106**, 241 (2017).
15. E. C. Gaudino, S. Tagliapietra, K. Martina, G. Palmisano and G. Cravotto, Recent Advances and Perspectives in the Synthesis of Bioactive Coumarins, *RSC Advances*., **6,** 46394 (2016).
16. M. Z. Hassan, H. Osman, M. A. Ali and M. J. Ahsan, Therapeutic Potential of Coumarins as Antiviral Agents, *Eur. J. Med. Chem*., **123**, 236 (2016).
17. L. Z. Chen, W. W. Sun, L. Bo, J. Q. Wang, C. Xiu, W. J. Tang and X. H. Liu, New Arylpyrazoline-Coumarins: Synthesis and Anti-inflammatory Activity, *Eur. J. Med. Chem*., **138**, 170 (2017).
18. T. Smyth, V. N. Ramachandran and W. F. Smyth, A Study of the Antimicrobial Activity of Selected Naturally Occurring and Synthetic Coumarins, *Int. J. Antimicrob. Agents*., **33**, 421 (2009).
19. S. Akoudad, S. K. L. Darweesh, M. J. G. Leening, P. J. Koudstaal, A. Hofman, A. Van Der Lugt and M. W Vernooij, Use of Coumarin Anticoagulants and Cerebral Microbleeds in the General Population, *Stroke*., **45**, 3436 (2009).
20. G. A. Gonçalves, A. R. Spillere, G. M. das Neves, L. P. Kagami, G. L. von Poser, R. F. S. Canto, and V. Eifler-Lima, Natural and Synthetic Coumarins as Antileishmanial Agents: A Review, *Eur. J. Med. Chem*., **203**, 112514 (2020).
21. T. Nasr, S. Bondock and M. Youns, Anticancer Activity of New Coumarin Substituted Hydrazide–Hydrazone Derivatives, *Eur. J. Med. Chem*., **76**, 539 (2014).
22. M. K. Gupta, S. Kumar and S, Chaudhary, Synthesis and Investigation of Antidiabetic Response of New Coumarin Derivatives against Streptozotocin Induced Diabetes in Experimental Rats. *Pharm, Chem. J*., **53**, 1122 (2020).
23. M. Yaseen, Z. Farooq, M. H. R. Mahmood, S. A. Ahmad, S. Nazir, K. M. Anjum and S. A. R. Naqvi, Synthesis of Novel Symmetric Porphyrin Schiff Base Dimers by Solid–Liquid Reaction Methodology. *J. Heterocycl. Chem.*, **56**, 1520 (2019).
24. S. K. Raju, A. Settu, A. Thiyagarajan, D. Rama, P. Sekar and S. Kumar, Biological Applications of Schiff Bases: An Overview. *GSC Biol. Pharm. Sci*. **21**, 203 (2022).
25. J. Ceramella, D. Iacopetta, A. Catalano, F. Cirillo, R. Lappano and M. S. Sinicropi, A Review on the Antimicrobial Activity of Schiff bases: Data Collection and Recent Studies, *Antibiotics*., **11**, 191 (2022).
26. Q. U. A. Sandhu, M. Pervaiz, A. Majid, U. Younas, Z. Saeed, A. Ashraf and S. Jelani, Review: Schiff Base Metal Complexes as Anti-inflammatory Agents, *J. Coord. Chem*., **76**, 1094 (2023).
27. A. D. Bagul, M. Kumar, A. M. Alanazi, A. Tufail, N. Tufail, D. D. Gaikwad and A. Dubey, Experimental and Computational Evaluation of Anti-malarial and Antioxidant Potential of Transition Metal (II) Complexes with Tridentate Schiff Base Derived from Pyrrolopyrimidine, *Biometals*., **37**, 1713 (2024).
28. H. Yalazan, D. Koç, F. Aydın Kose, S. Fandaklı, B. Tüzün, M. İ. Akgül, N. Sadeghiane, P. Taslimi and H. kantekin, Design, Syntheses, Theoretical Calculations, MM-GBSA, Potential Anti-cancer and Enzyme Activities of Novel Schiff Base Compounds, *J. Biomol. Struct. Dyn*., **42**, 13100 (2024).
29. W. U. Islam, A. Khan, F. Khan, S. Ullah, M. Waqas, H. Khan, M. Khan, S. M. Rahman, S. Ali, A. Mateen, A, Khalid, A. Khan and A. Al-Harrasi , Synthesis of Novel Hydrazide Schiff Bases with Anti-diabetic and Anti-hyperlipidemic Effects: *In-Vitro* , *In-Vivo* and *In-Silico* Approaches, *J. Biomol. Struct. Dyn*., **1**, 12 (2024).
30. A.- Wahab, F. Nadeem, U. Salar, H. M. Bilal, M. Farooqui, S. Javaid, S. Sadaf, K. M, Khan and M. I. Choudhary, Coumarin Derivatives as New Anti-biofilm Agents Against *Staphylococcus aureus*, *Plos One*., **19**, e0307439 (2024).
31. S. B. Zahra, S. Ullah, S. A. Halim, M. Waqas, N. U. Huda, A. Khan, A. Y. Binsaleh, A. F. El-Kott, J. Hussain, A. Al-Harrasi and Z. Shafiq, Synthesis of Novel Coumarin-Based Thiosemicarbazones and Their Implications in

Diabetic Management *via In-Vitro* and *In-Silico* Approaches, *Sci. Rep*., **13**, 18014 (2023).

32. T. M. Sharanakumar, V. K. A. Kalalbandi, K. N. Shashiraj, K. M. Nagarsha and H. M. Babu, Studies on Novel Metal Complexes of Coumarin Schiff Base: Synthesis, Stability Constant, Antimicrobial, and Anticancer Activity, *Rasayan J. Chem*., **17**, 945 (2023).
33. V. N. Toan and N. D. Thanh, Synthesis and Antiproliferative Activity of Hybrid Thiosemicarbazone Derivatives Bearing Coumarin and D-galactose Moieties with EGFR Inhibitory Activity and Molecular Docking Study, *Med. Chem. Res*., **30**, 1868 (2021).
34. S. Tighadouni, S. Radi, M. Sirajuddin, M. Akkurt, N. Özdemir, M. Ahmad, Y. N. Mabkhot and T. B. Hadda, *In Vitro* Antifungal, Anticancer Activities and POM Analyses of a Novel Bioactive Schiff Base 4-{[(E)-Furan-2-ylmethylidene]Amino}*p*-Henol: Synthesis, Characterization and Crystal Structure, *J. Chem. Soc. Pak*., **38**, (2016).
35. K. A. Dahlous, M. Ajmal, S. Ullah, A. Khan, M. al-Rashida, T. Islam, Z. Xianliang, F. Noreen, N. Ahmed, A. Al-Harrasi and Z. Shafiq, Design, Synthesis, *In-Vitro* and *In-Silico* Studies of 6-Bromochromone Based Thiosemicarbazones as α-Glucosidase Inhibitors, *J. Mol. Struct*., **1329**, 141374 (2025).
36. R. D. Alharthy, S. Khalid, S. Fatima, S. Ullah, A. Khan, S. N. Mali, R. D. Jawarkar. S. S. Dhabarde, H. Kashtoh, P. Taslimi, A. Al-Harrasi, Z. Shafiq and N. M. Boshta, Synthesis of the Chromone-Thiosemicarbazone Scaffold as Promising α-Glucosidase Inhibitors: An *In Vitro* and *In Silico* Approach toward Antidiabetic Drug Design, *Arch. Pharm.*, **357**, 2400140 (2024).
37. F. Noreen, S. Ullah, S. N. Mali, A. Khan, J. Hussain, A. Alshammari, N. A. Albekairi, R. D. Jawarkar, S. Yadav, A. Al-Harrasi and Z. Shafiq, Synthesis, *In Vitro*, and *In Silico* Studies of 7-Fluorochromone Based Thiosemicarbazones as α-Glucosidase Inhibitors, *Sci. Rep*., **15**, 9816 (2025).
38. E. Çelik, M. Özdemir, B. Köksoy, T. Taskin-Tok, P. Taslimi, N. Sadeghian and B. Yalcin, New Coumarin−Thiosemicarbazone Based Zn(II), Ni(II) and Co(II) Metal Complexes: Investigation of Cholinesterase, α-Amylase, and α-Glucosidase Enzyme Activities, and Molecular Docking Studies, *Chem. Select*., **8**, e202301786 (2023).
39. U. Salar, K. M. Khan, S. Chigurupati, S. Syed, S. Vijayabalan, A. Wadood, M. Riaz, M. Ghufran and S. Perveen, New Hybrid Scaffolds Based on Hydrazinyl Thiazole Substituted Coumarin; As Novel Leads of Dual Potential; *In Vitro* α-Amylase Inhibitory and Antioxidant (DPPH and ABTS Radical Scavenging) Activities, *Med. Chem*., **15**, 87 (2019).
40. W. Zareen, N. Ahmed, A. M. Khan, S. N. Mali, N. Sadeghian, N. A. Aldawsari, P. Taslimi, A. K. Alanazi, M. Tahir, M. Tasleem and Z. Shafiq, Synthesis, Antidiabetic Evaluation, and Computational Modeling of 3-Acetyl-8-Ethoxy Coumarin Derived Hydrazones and Thiosemicarbazones, *RSC Adv*., **15**, 39043 (2025).
41. L. T. Theunis, J. B. Billones, C.-D. Hsiao, O. B. Villaflores and A. L. Llamasares-Castillo, *In Silico*, *In Vitro*, and *In Vivo* Evaluation of the Anti-alzheimer's Activity of Berberine, *CEI*. **20**, 199 (2024).
42. U. Zahra, S. Zaib, A. Saeed, M. ur Rehman, G. Shabir, H. O. Alsaab and I. Khan, New Acetylphenol-Based Acyl Thioureas Broaden the Scope of Drug Candidates for Urease Inhibition: Synthesis, *In Vitro* Screening and *In Silico* Analysis, *Int. J. Biol. Macromol*., **198**, 157 (2022).
43. M. Taha, M. S. Baharudin, N. H. Ismail, S. Imran, M. N. Khan, F. Rahim and S. Vijayabalan, Synthesis, α-Amylase Inhibitory Potential and Molecular Docking Study of Indole Derivatives, *Bioorg. Chem*., **80**, 36 (2018).
44. M. Hassan, A. Rasul, F. Jabeen, S. Sultana and M. Manan, Bombax Ceiba Extract and its Metabolites as α-Glucosidase Inhibitors for Diabetes, *J. King Saud Univ. Sci*., **36**, 103267 (2024).
45. M. Akash, N. Rana, S. Aslam, M. Ahmad, M. J. Saif, A. Asghar, S. Sultan, S. A. Al-Hussain, A. Liaqat, S. Zaib and M. E. A. Zaki, Pyridylpiperazine-Based Carbodithioates as Urease Inhibitors: Synthesis and Biological Evaluation, *Front. Chem*., **12**, 1423385 (2024).
46. F. A. Saddique, M. Ahmad, U. A. Ashfaq, A. Mansha and S. G. Khan, Alpha-Glucosidase Inhibition and Molecular Docking Studies of 4-Hydroxy-n'-[Benzylidene/1-Phenylethylidene]-2*H*-1,2-Benzothiazine-3-Carbohydrazide 1,1-Dioxides, *Chiang Mai J. Sci*., **48**, 460 (2021).
47. D. S. Ranade, A. M. Bapat, S. N. Ramteke, B. N. Joshi, P. Roussel, A. Tomas, P. Deschamps and P. P. Kulkarni, Thiosemicarbazone Modification of 3-Acetyl Coumarin Inhibits Aβ Peptide Aggregation and Protect Against Aβ-induced Cytotoxicity, *Eur. J. Med. Chem*., **121**, 803 (2016).

48. A. Agarkov, A. Nefedova, A. Ovsyannikov, I. Litvinov, S. Solovieva and I. Antipin, Synthesis and Crystal Structure of Ethyl 5-(4-Bromophenyl)-7-Methyl-3-oxo-2,3-Dihidro-5*H*-Thiazolo[3,2-*a*]Pyrimidine-6-Carboxylate, *Molbank*., **1**, 1581 (2023).
49. M. Akash, S. Zaib, M. Ahmad, S. Sultan and S. A. Al-Hussain, Synthesis and Biological Evaluation of Pyridylpiperazine Hybrid Derivatives as Urease Inhibitors, *Front. Chem*., **12**, 1371377 (2024).
50. U. M. Osman, S. Silvarajoo, M. F. Noor Hassim, S. Arshad, A. H. Anizaim and F. I. A. Razak, Synthesis, X-Ray Structure, Hirshfeld Surface Analysis, DFT Calculations, and Molecular Docking Studies of Nickel(II) Complex with Thiosemicarbazone Derivative, *Bioinorg. Chem. Appl*., **1**, 5536902 (2021).
51. M. Yaseen, Z. Farooq, M. Ahmad, M. A. Sultan, M. A. Raza, J. Y. Winum, M. Mustafa, M. HR. Mahmood, M, Tayyab, M. A. Iqbal and M. S. Mahr, Synthesis and Investigation of Linear and Nonlinear Optical Properties of an Octahedral Metalloporphyrin, *Opt. Mater*., **149**, 115092 (2024).
52. M. Yaseen, M. Awais, Z. Farooq, M. Ahmad, J. Y. Winum, M. Mustafa, G. M. Mustafa, M. HR. Mahmood and M Latif, Green Synthesis, Structural Tailoring, and Optical Optimization of Porphyrins for High-Performance Thin Film Resistive-Capacitive Sensors, *J. Mol. Struct*., **1335**, 141985 (2025).
53. M. A. Marzouk, M. M. Elsayed, W. S. Shehab, S. M. Fawzy, S. M. Mohammed, M. A. Abdel-Razek, G. E. Khedr and D. A. Elsayed, Dual α-Amylase and α-Glucosidase Inhibition by 1,2, 4-Triazole Derivatives for Diabetes Treatment, *Sci. Rep*., **15**, 27172 (2025).
54. P. Garg, H. S. Bhatt, S. K. Roy and S. R. Reddy, α-Amylase Inhibitory Potential of Dihydropyrano Coumarins: *In Silico* and DFT Analysis, *3 Biotech*., **15**, 38 (2025).